

Seasonal variations in aerosol optical properties over China

Yuesi Wang,¹ Jinyuan Xin,¹ Zhanqing Li,² Shigong Wang,³ Pucai Wang,¹ Wei Min Hao,⁴ Bryce L. Nordgren,⁴ Hongbin Chen,¹ Lili Wang,¹ and Yang Sun¹

Received 23 November 2010; revised 17 June 2011; accepted 14 July 2011; published 28 September 2011.

[1] Seasonal variations in background aerosol optical depth (AOD) and aerosol type are investigated over various ecosystems in China based upon three years' worth of meteorological data and data collected by the Chinese Sun Hazemeter Network. In most parts of China, AODs are at a maximum in spring or summer and at a minimum in autumn or winter. Minimum values (0.10~0.20) of annual mean AOD at 500 nm are found in the Qinghai-Tibetan Plateau, the remote northeast corner of China, the northern forest ecosystems and Hainan Island. Annual mean AOD ranges from 0.25 to 0.30 over desert and oasis areas, as well as the desertification grasslands in northern China; the annual mean AOD over the Loess Plateau is moderately high at 0.36. Regions where the highest density of agricultural and industrial activities are located and where anthropogenic sulphate aerosol and soil aerosol emissions are consistently high throughout the whole year (e.g., the central-eastern, southern and eastern coastal regions of China) experience annual mean AODs ranging from 0.50~0.80. Remarkable seasonal changes in the main types of aerosol over northern China (characterized by the Angstrom exponent, α) are seen. Due to biomass and fossil fuel burning from extensive agricultural practices in northern rural areas, concentrations of smoke and soot aerosols rise dramatically during autumn and winter (high α), while the main types of aerosol during spring and summer are dust and soil aerosols (low α). Over southeastern Asia, biomass burning during the spring leads to increases in smoke and soot emissions. Over the Tibetan Plateau and Hainan Island where the atmosphere is pristine, the main types of aerosol are dust and sea salt, respectively.

Citation: Wang, Y., J. Xin, Z. Li, S. Wang, P. Wang, W. M. Hao, B. L. Nordgren, H. Chen, L. Wang, and Y. Sun (2011), Seasonal variations in aerosol optical properties over China, *J. Geophys. Res.*, 116, D18209, doi:10.1029/2010JD015376.

1. Introduction

[2] Under the aegis of the East Asian Study of Tropospheric Aerosols – an International Regional Experiment (EAST-AIRE) [Li *et al.*, 2007b], the Chinese Sun Hazemeter Network (CSHNET) was successfully implemented to obtain spatial and temporal distributions of aerosol optical properties in China [Xin *et al.*, 2006, 2007]. This paper uses long-term network data and synchronous meteorological data to examine the seasonal variability of aerosol optical properties, size, composition and sources throughout China. This work will help reduce uncertainties regarding aerosol optical properties over the Chinese continent. Section 2

describes the data and methodology used and section 3 presents the results from analyses of aerosol optical properties measured at sites located in the six different ecosystems studied here. Conclusions are given in section 4.

[3] China is situated in the eastern part of Asia, on the west coast of the Pacific Ocean. It is the third largest country in the world, comprising about 6.7% of the world's total land area, and is home to 22% of the world's human population. From arid deserts to tropical forests and from the Qinghai-Tibet Plateau to immense plains and the seashore, China contains a variety of ecosystems. The vast Chinese mainland is one of the major global aerosol sources. During the past few decades, Chinese dramatic increases in large-scale farming, urbanization and industrial activities may aggravate the uncertainty of aerosol climate and radiation effects in the region [Penner *et al.*, 2001; Forster *et al.*, 2007; Huebert *et al.*, 2003; Li, 2004; Seinfeld *et al.*, 2004]. Substantially more coal and biomass burning events and dust storms occur in China, adding more absorbing soot and organic aerosols into the Asian and Pacific atmospheres [Lelieveld *et al.*, 2001; Streets *et al.*, 2001, 2003, 2004; Eck *et al.*, 2005; Streets and Aunan, 2005; Seinfeld *et al.*, 2004]. Lee *et al.* [2007] suggested that the aerosols in China have a significant impact on the

¹LAPC, Institute of Atmospheric Physics, Chinese Academy of Sciences, Beijing, China.

²Department of Atmospheric and Oceanic Sciences, University of Maryland, College Park, Maryland, USA.

³College of Atmospheric Science, Lanzhou University, Lanzhou, China.

⁴Fire Sciences Laboratory, USDA Forest Service, Missoula, Montana, USA.

Table 1. The Annual and Seasonal Means and Standard Deviations of Aerosol Optical Depth (AOD) at 500 nm and Angstrom Exponent (α) Measured at the CSHNET Regional Background Sites

Site	Annual Mean		Spring		Summer		Autumn		Winter	
	AOD	α								
<i>Northeastern China</i>										
Sanjiang	0.21 ± 0.09	1.28 ± 0.61	0.27 ± 0.12	0.96 ± 0.15	0.24 ± 0.07	0.64 ± 0.14	0.20 ± 0.06	1.35 ± 0.50	0.15 ± 0.03	1.90 ± 0.58
Hailun	0.18 ± 0.05	1.96 ± 0.53	0.20 ± 0.05	1.84 ± 0.28	0.19 ± 0.04	1.36 ± 0.61	0.13 ± 0.01	2.33 ± 0.37	0.19 ± 0.04	2.23 ± 0.33
Changbai Mt.	0.22 ± 0.09	1.17 ± 0.43	0.26 ± 0.09	0.87 ± 0.21	0.30 ± 0.07	0.84 ± 0.28	0.15 ± 0.04	1.39 ± 0.39	0.16 ± 0.02	1.54 ± 0.35
Shenyang	0.49 ± 0.13	0.93 ± 0.28	0.53 ± 0.11	0.76 ± 0.17	0.55 ± 0.21	0.69 ± 0.27	0.45 ± 0.07	1.15 ± 0.24	0.45 ± 0.06	1.08 ± 0.16
<i>An Arid Region in Northern China</i>										
Fukang	0.29 ± 0.11	0.96 ± 0.28	0.25 ± 0.03	0.78 ± 0.20	0.25 ± 0.03	0.82 ± 0.17	0.23 ± 0.06	1.21 ± 0.24	0.42 ± 0.14	1.01 ± 0.27
Ordos	0.27 ± 0.10	0.47 ± 0.37	0.35 ± 0.08	0.21 ± 0.14	0.31 ± 0.13	0.35 ± 0.41	0.20 ± 0.04	0.50 ± 0.27	0.21 ± 0.06	0.85 ± 0.36
Shapotou	0.32 ± 0.09	0.90 ± 0.28	0.36 ± 0.11	0.65 ± 0.22	0.31 ± 0.11	0.88 ± 0.25	0.29 ± 0.06	0.98 ± 0.27	0.32 ± 0.07	1.06 ± 0.24
Ansai	0.36 ± 0.11	0.86 ± 0.60	0.47 ± 0.09	0.42 ± 0.26	0.33 ± 0.06	0.21 ± 0.24	0.31 ± 0.08	1.08 ± 0.29	0.32 ± 0.11	1.57 ± 0.45
<i>The Tibetan Plateau</i>										
Haibei	0.13 ± 0.05	0.82 ± 0.51	0.17 ± 0.05	0.33 ± 0.31	0.18 ± 0.03	0.62 ± 0.41	0.11 ± 0.03	1.25 ± 0.32	0.10 ± 0.04	1.04 ± 0.42
Lhasa	0.15 ± 0.04	-0.15 ± 0.25	0.19 ± 0.03	-0.18 ± 0.28	0.17 ± 0.02	-0.21 ± 0.32	0.13 ± 0.02	-0.16 ± 0.21	0.12 ± 0.02	-0.06 ± 0.21
<i>Forest Ecosystem</i>										
Beijing Forest	0.22 ± 0.09	0.82 ± 0.39	0.29 ± 0.10	0.55 ± 0.25	0.27 ± 0.08	0.62 ± 0.24	0.18 ± 0.07	0.93 ± 0.30	0.15 ± 0.04	1.20 ± 0.41
Dinghu Mt.	0.66 ± 0.21	1.00 ± 0.41	0.80 ± 0.20	1.21 ± 0.48	0.56 ± 0.24	1.31 ± 0.52	0.69 ± 0.15	0.78 ± 0.20	0.59 ± 0.24	0.86 ± 0.25
Xishuangbanna	0.45 ± 0.17	1.34 ± 0.39	0.61 ± 0.15	1.60 ± 0.23	0.34 ± 0.13	0.91 ± 0.40	0.37 ± 0.10	1.21 ± 0.32	0.44 ± 0.15	1.55 ± 0.20
<i>Farmland Ecosystem</i>										
Fengqiu	0.56 ± 0.14	1.08 ± 0.18	0.62 ± 0.09	0.92 ± 0.19	0.71 ± 0.10	1.07 ± 0.09	0.50 ± 0.10	1.13 ± 0.14	0.45 ± 0.13	1.22 ± 0.13
Taoyuan	0.69 ± 0.17	1.04 ± 0.14	0.70 ± 0.10	0.92 ± 0.12	0.60 ± 0.13	0.94 ± 0.06	0.73 ± 0.23	1.12 ± 0.12	0.70 ± 0.18	1.14 ± 0.11
Yanting	0.79 ± 0.17	1.02 ± 0.15	0.93 ± 0.10	0.92 ± 0.19	0.81 ± 0.07	1.11 ± 0.11	0.67 ± 0.19	1.03 ± 0.15	0.76 ± 0.16	1.05 ± 0.08
<i>Bay and Lake Ecosystems</i>										
Jiaozhou Bay	0.64 ± 0.13	1.16 ± 0.19	0.70 ± 0.08	1.05 ± 0.19	0.79 ± 0.08	1.05 ± 0.18	0.57 ± 0.12	1.31 ± 0.15	0.53 ± 0.07	1.20 ± 0.11
Lake Tai	0.45 ± 0.09	0.80 ± 0.24	0.43 ± 0.08	0.77 ± 0.25	0.59 ± 0.03	0.73 ± 0.46	0.49 ± 0.07	0.93 ± 0.11	0.39 ± 0.09	0.88 ± 0.19
Sanya Bay	0.23 ± 0.10	0.39 ± 0.38	0.26 ± 0.06	0.61 ± 0.28	0.22 ± 0.09	-0.04 ± 0.24	0.20 ± 0.12	0.32 ± 0.26	0.21 ± 0.12	0.50 ± 0.39

accuracy of the hazemeters. Vaisala M520 automatic meteorological stations provide the surface (2-m) measurements of meteorological parameters, such as wind speed, temperature and humidity, at the CERN sites.

[7] A log linear fitting was applied to AODs at three wavelengths (405 nm, 500 nm and 650 nm) [Kim *et al.*, 2004] to estimate the Angstrom exponent (α), a basic parameter related to the aerosol size distribution. In general, α ranges from 0.0 to 2.0, with the smaller α corresponding to larger aerosol particle sizes [Dubovik *et al.*, 2002; Kim *et al.*, 2004]. Daily AOD, α and temperature (T) are averaged from 10 A.M. to 2 P.M. (local time). The highest local wind speed (V_{\max}) and the wind direction are defined as the mean of the highest wind speeds and wind directions measured over each hour from 10 A.M. to 2 P.M. (local time).

[8] The network stations are located in different climate zones over the vast territory of China (Figure 1). Changbai Mountain (temperate forest), Hailun (farmland), Sanjiang (marsh/farmland) and Shenyang (suburban farmland) are temperate continental monsoon climate with windy spring, warm rainy summer, fine autumn and cold dry winter. Fukang (oasis), Ordos (sandy grassland) and Shapotou (desert) are temperate desertification climate with windy spring, hot summer and cold winter. Ansai (forest, grassland and farmland) is located in the transition zone between semi-arid and semi-humid temperate continental climate. Haibei (alpine meadow) and Lhasa (alpine shrub-grassland) are Qinghai-Tibet plateau Alpine-cold climate with dry windy spring and winter, nice and cool humid summer and autumn. Beijing Forest is a warm temperate forest ecosystem to the

west of Beijing City with the typical temperate semi-humid monsoon climate. Dinghu Mountain is a subtropical evergreen forest ecosystem in the Pearl River delta region, with subtropical monsoon humid climate. Xishuangbanna is a tropical rain forest ecosystem in Yunnan Province with tropical monsoon climate, dry and humid season. Fengqiu (farmland) is located in the Huang-huai-hai Plain with semi-arid and semi-humid temperate monsoon climate. Taoyuan (subtropical farmland) is located in the transition zone between central and northern subtropical monsoon climate. Yanting (farmland) is located in the hilly region of the Sichuan Basin, with central subtropical monsoon climate. Jiaozhou Bay is on the west coast of the Yellow Sea with temperate climate. Lake Tai is a freshwater lake in the Yangtze River Delta region with northwest and southeast monsoon climate. Sanya Bay is a tropical marine bay in the South China Sea with tropical monsoon climate.

3. Results and Discussion

[9] The annual and seasonal mean values of monthly AOD and α for the 19 CERN sites are listed in Table 1, and the means and standard deviations of daily AOD and α under different wind speed and directions (East: 45°~135°, South: 135°~225°, West: 225°~315°, North: 315°~360° and 0°~45°) in Table 2. It should be noted that the mean values for the same site in Tables 1 and 2 are not comparable because their denominators are different.

Table 2. The Means and Standard Deviations of Aerosol Optical Depth (AOD) at 500 nm and Angstrom Exponent (α) Under Different Wind Speed and Directions at the CSHNET Regional Background Sites^a

Site	Wind Speed						Wind Direction							
	<5m/s		5–10m/s		>10m/s		East		South		West		North	
	Percent	AOD	Percent	AOD	Percent	AOD	Percent	AOD	Percent	AOD	Percent	AOD	Percent	AOD
<i>Northeastern China</i>														
Sanjiang	59%	0.17 ± 0.111.62 ± 0.75	39%	0.16 ± 0.101.86 ± 1.73	2%	0.19 ± 0.111.53 ± 0.90	4%	0.24 ± 0.141.17 ± 0.55	25%	0.21 ± 0.131.64 ± 0.71	64%	0.15 ± 0.081.83 ± 0.77	7%	0.22 ± 0.121.27 ± 0.39
Hailun	52%	0.18 ± 0.072.09 ± 0.61	46%	0.17 ± 0.192.38 ± 0.67	3%	0.14 ± 0.092.34 ± 0.71	6%	0.23 ± 0.081.59 ± 0.30	21%	0.20 ± 0.081.94 ± 0.60	47%	0.15 ± 0.082.41 ± 0.57	26%	0.17±0.23 2.29 ± 0.74
Changbai Mt.	87%	0.18 ± 0.101.41 ± 0.61	13%	0.14 ± 0.091.39 ± 0.57			3%	0.17 ± 0.080.82 ± 0.62	11%	0.18 ± 0.091.24 ± 0.40	69%	0.17 ± 0.101.51 ± 0.61	0.16%	0.20 ± 0.111.21 ± 0.54
Shenyang	57%	0.47 ± 0.241.08 ± 0.37	39%	0.48 ± 0.260.99 ± 0.37	3%	0.49 ± 0.321.02 ± 0.49	13%	0.50 ± 0.251.07 ± 0.33	36%	0.53 ± 0.281.02 ± 0.39	21%	0.45 ± 0.251.08 ± 0.40	29%	0.42 ± 0.201.03 ± 0.35
<i>An Arid Region in Northern China</i>														
Fukang	68%	0.25 ± 0.161.15 ± 0.46	31%	0.21 ± 0.101.04 ± 0.45	1%	0.22 ± 0.070.74 ± 0.08	55%	0.24 ± 0.161.16 ± 0.52	8%	0.27 ± 0.171.07 ± 0.34	28%	0.24 ± 0.101.06 ± 0.36	9%	0.23 ± 0.131.06 ± 0.41
Ordos	45%	0.20 ± 0.131.05 ± 0.76	51%	0.25 ± 0.180.70 ± 0.68	4%	0.29 ± 0.250.54 ± 0.68	9%	0.26 ± 0.160.81 ± 0.54	16%	0.30 ± 0.200.75 ± 0.46	46%	0.21 ± 0.170.87 ± 0.82	29%	0.21 ± 0.140.87 ± 0.80
Shapotou	58%	0.35 ± 0.140.92 ± 0.35	40%	0.34 ± 0.140.73 ± 0.34	2%	0.36 ± 0.160.38 ± 0.26	34%	0.39 ± 0.140.84 ± 0.26	9%	0.31 ± 0.140.91 ± 0.32	28%	0.29 ± 0.130.82 ± 0.50	29%	0.34 ± 0.140.81 ± 0.33
Ansai	92%	0.32 ± 0.191.42 ± 0.82	8%	0.37 ± 0.260.99 ± 0.79			23%	0.31 ± 0.261.19 ± 0.78	22%	0.41 ± 0.191.16 ± 0.65	3%	0.26 ± 0.061.49 ± 1.07	52%	0.29 ± 0.171.54 ± 0.86
<i>The Tibetan Plateau</i>														
Haibei	40%	0.11 ± 0.061.61 ± 0.86	53%	0.16 ± 0.081.21 ± 0.99	6%	0.16 ± 0.101.16 ± 1.04	15%	0.13 ± 0.071.53 ± 0.84	18%	0.16 ± 0.081.44 ± 0.88	32%	0.14 ± 0.081.28 ± 1.05	35%	0.13 ± 0.081.34 ± 0.97
Lhasa	73%	0.11 ± 0.070.10 ± 0.44	25%	0.11 ± 0.050.16 ± 0.42	2%	0.13 ± 0.060.08 ± 0.51	33%	0.12 ± 0.090.07 ± 0.45	13%	0.13 ± 0.040.00 ± 0.38	41%	0.09 ± 0.040.23 ± 0.43	13%	0.13 ± 0.05-0.02 ± 0.39
<i>Forest Ecosystem</i>														
Beijing Forest	50%	0.20 ± 0.161.43 ± 0.79	46%	0.20 ± 0.191.24 ± 0.67	4%	0.12 ± 0.071.38 ± 0.80	14%	0.25 ± 0.171.33 ± 0.62	9%	0.20 ± 0.131.16 ± 0.72	41%	0.21 ± 0.201.16 ± 0.67	36%	0.16 ± 0.131.59 ± 0.80
Dinghu Mt.	88%	0.64 ± 0.290.82 ± 0.29	12%	0.59 ± 0.230.92 ± 0.31			9%	0.58 ± 0.220.83 ± 0.23	23%	0.55 ± 0.200.88 ± 0.30	17%	0.58 ± 0.270.86 ± 0.36	52%	0.69 ± 0.320.80 ± 0.28
Xishuangbanna	100%	0.45 ± 0.241.59 ± 0.61					17%	0.47 ± 0.281.64 ± 0.55	27%	0.41 ± 0.221.65 ± 0.66	42%	0.48 ± 0.251.59 ± 0.59	13%	0.41 ± 0.171.38 ± 0.64
<i>Farmland Ecosystem</i>														
Fengqiu	65%	0.57 ± 0.251.09 ± 0.27	35%	0.55 ± 0.300.92 ± 0.28			5%	0.60 ± 0.211.02 ± 0.31	41%	0.66 ± 0.261.07 ± 0.24	23%	0.38 ± 0.181.08 ± 0.30	32%	0.56 ± 0.280.95 ± 0.30
Taoyuan	96%	0.70 ± 0.301.02 ± 0.26	4%	0.83 ± 0.400.99 ± 0.28			41%	0.76 ± 0.281.02 ± 0.26	19%	0.63 ± 0.300.96 ± 0.25	32%	0.63 ± 0.301.05 ± 0.26	7%	0.91 ± 0.331.05 ± 0.20
Yanting	98%	0.85 ± 0.370.96 ± 0.27	2%	0.72 ± 0.210.38 ± 0.22			44%	0.87 ± 0.370.96 ± 0.28	19%	0.91 ± 0.370.99 ± 0.25	21%	0.86 ± 0.350.92 ± 0.28	15%	0.70 ± 0.370.92 ± 0.28
<i>Bay and Lake Ecosystems</i>														
Jiaozhou Bay	22%	0.72 ± 0.281.23 ± 0.26	55%	0.63 ± 0.321.22 ± 0.30	23%	0.56 ± 0.371.17 ± 0.34	8%	0.71 ± 0.271.11 ± 0.24	35%	0.72 ± 0.331.21 ± 0.30	26%	0.58 ± 0.311.21 ± 0.31	32%	0.58 ± 0.331.23 ± 0.31
Lake Tai	40%	0.44 ± 0.101.02 ± 0.20	54%	0.42 ± 0.130.93 ± 0.25	6%	0.39 ± 0.130.80 ± 0.39	19%	0.47 ± 0.150.97 ± 0.22	40%	0.42 ± 0.100.98 ± 0.23	18%	0.42 ± 0.130.91 ± 0.21	24%	0.40 ± 0.110.95 ± 0.31
Sanya Bay	87%	0.23 ± 0.170.32 ± 0.48	13%	0.27 ± 0.140.54 ± 0.39			60%	0.22 ± 0.160.44 ± 0.42	22%	0.24 ± 0.200.13 ± 0.55	15%	0.26 ± 0.150.23 ± 0.48	3%	0.26 ± 0.100.74 ± 0.33

^aEast: 45°–135°, South: 135°–225°, West: 225°–315°, North: 315°–360° and 0°–45°.

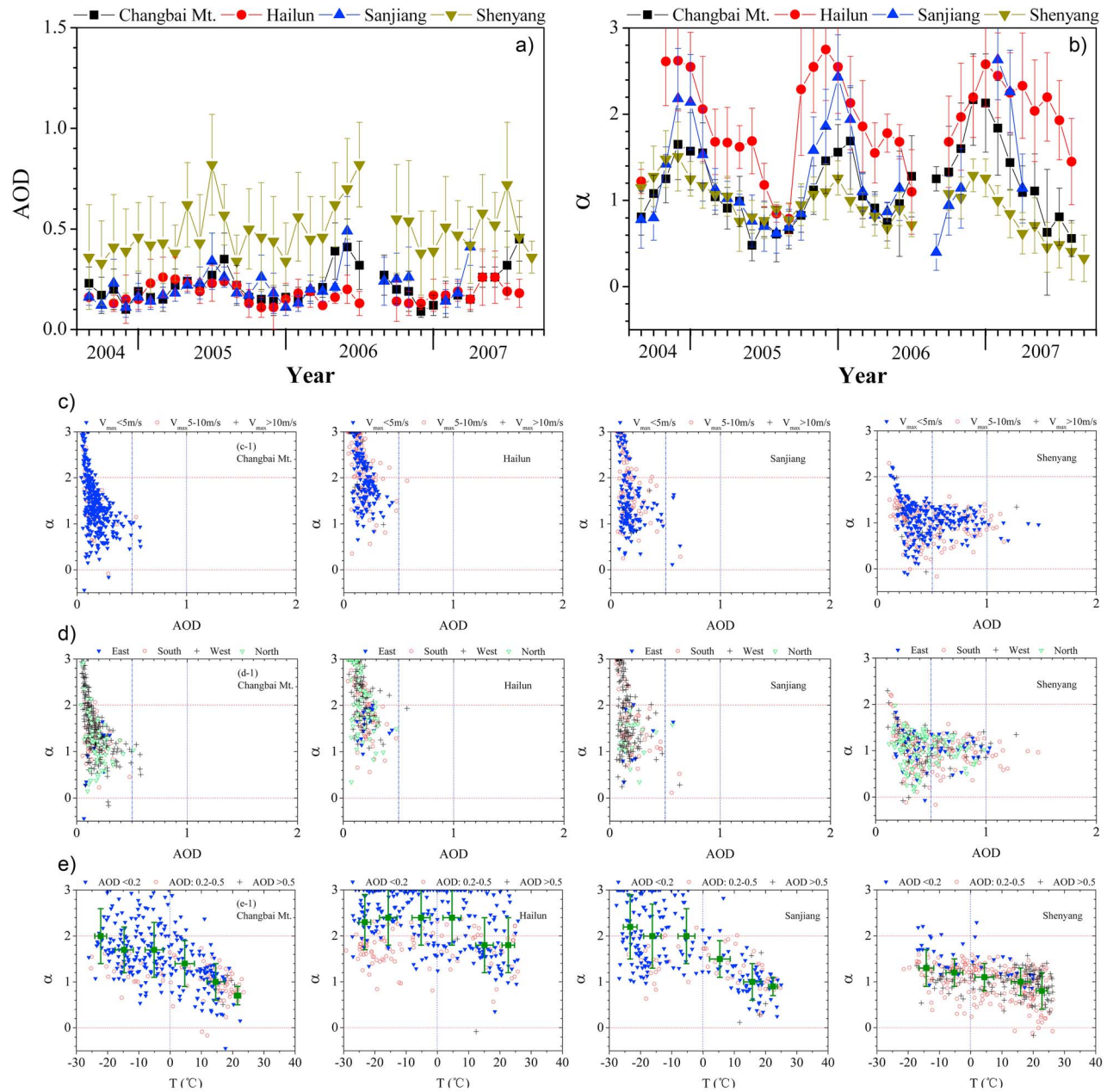


Figure 2. Seasonal variations in monthly averaged (a) AOD at 500 nm and (b) α , (c) α as a function of AOD with wind speed and (d) with wind directions (East: 45°~135°, South: 135°~225°, West: 225°~315°, North: 315°~360° and 0°~45°), (e) α as a function of temperature at the four CERN sites in northeastern China. The sites are Changbai Mountain (temperate forest), Hailun (farmland), Sanjiang (marsh/farmland) and Shenyang (suburban farmland). The green squares in Figure 2e represent mean α/T over each 10°C-T bin.

3.1. Northeastern China

[10] Figures 2a and 2b show a marked seasonal cycle in the monthly averaged AOD at 500 nm and the monthly averaged α from August 2004 to August 2007 in northeastern China. The scatterplots of α as a function of AOD (Figure 2c), which are classified according to V_{max} , show that V_{max} has no influence on the relationship between α and AOD. The scatterplots of α and AOD in different wind speed range are used to conjecture the differences of aerosol

optical properties from the local, near and the far area. The functions of α and AOD are accordant in different wind speed, which implies the observation site has good representative in the region [Lewis and Schwartz, 2004; Seinfeld and Pandis, 1998]. At the Shenyang site, a suburban agricultural site 35 km south of Shenyang City in northeastern China, the annual mean and standard deviation of AOD and α are 0.49 ± 0.13 and 0.93 ± 0.28 , respectively. Remote sites in northeastern China, such as Sanjiang, Hailun and

Changbai Mt., have clean air so the annual mean AOD is low, ranging from 0.18 to 0.22; the annual mean α ranges from 1.17 to 1.96 at these sites. The Northeast China is characterized by a temperate continental monsoon climate with warm and wet summer and cold and dry winter. The scatterplots of α and AOD under different wind directions (Figure 2d) and Table 2 show that the aerosol properties were different under dominant wind directions in different seasons. The easterly and southerly winds always occurred in summer with low speed and relative high humidity to accumulate the particle matter in the region. The westerly and northerly winds were strong and clean with low AOD to sweep the regional pollutant away not in winter and spring but in summer and autumn. The scatterplots of α as a function of T (Figure 2e) show that α increased with T decreasing when AOD < 0.5 and that the mean T (green squares, especially at the remote Changbai Mt. and Sanjiang sites) experiences the same change, which implies a systematic seasonal shift in aerosol type. The aerosol particle size decreases from autumn to winter, reflecting such activities as the agricultural practice of burning crop stalks in autumn and the increase in fossil fuel and biomass burning for heating as the winter season approaches [Cao *et al.*, 2005]. Also, a ginseng plantation is located in the Changbai Mt. region and burning grass is a traditional way to prepare the land for planting ginseng during the fall [Yu *et al.*, 1999]. Meanwhile, a gradual increase in snow and ice cover on the ground prevents soil erosion and thus restricts the emission of coarse-mode mineral particles, which is also suggested by the low AOD loading during the winter season. An opposite trend is observed from winter to spring and summer when AOD values increased and α decreased. In spring and summer, the aerosols seem to be more of a continental type due to regional dust transmission and local soil emission. In addition, the influences of rural biomass burning (Figure 2e, second plot, at Hailun) and urban pollutant emission (Figure 2e, fourth plot, at Shenyang) on aerosol properties are very significant.

3.2. Arid Region of North China

[11] Figure 3 is the same as Figure 2 but for arid and semi-arid regions of northern China. The annual mean AOD and α (Figures 3a and 3b) show similar seasonal variations and range from 0.27 to 0.37 and from 0.47 to 0.96, respectively. AODs and atmospheric turbidity are larger over the desert (Shapotou) and arid agricultural (Ansai) sites than at the other two sites. Because the sole source of aerosols in the more desert-like region is natural dust emission, dust aerosols are more dominant at the Shapotou site [Gai *et al.*, 2006; Xin *et al.*, 2005]. The mean α are 0.92 ± 0.35 , 0.73 ± 0.34 and 0.38 ± 0.26 when $V_{\max} < 5$ m/s, 5 m/s < $V_{\max} < 10$ m/s and $V_{\max} > 10$ m/s, respectively. The scatterplots (Figure 3c) and the mean α and AOD (Table 2) with different wind speed show that more large aerosol particles appear with increasing wind speed, which suggests that powerful winds blow local large dust particles into the atmosphere in this part of China [Alfaro *et al.*, 2003; Xia *et al.*, 2004; Xin *et al.*, 2005]. There is not significant difference in the scatterplots (Figure 3d) but there is difference in the mean AODs (Table 2) with different wind directions. The southerly wind at Fukang, the easterly and southerly winds at Ordos and Ansai, the easterly and northerly winds at Shapotou carried a

certain amount of aerosol from the upwind region where some towns and countries strew over. The westerly and northerly winds are always clean with low AOD. The scatterplots of α as a function of T (Figure 3e) show that α increases with T decreasing when AOD < 0.5, which indicates the presence of background smoke aerosols in autumn and winter due to biomass burning by the farmer in the north-west wide part of China [Cao *et al.*, 2005].

3.3. The Tibetan Plateau

[12] Analysis of aerosol optical properties at two sites located on the Tibetan Plateau is shown in Figure 4. The two sites, Haibei and Lhasa, are located in alpine meadow and alpine shrub-grassland ecosystems, respectively, where some level of livestock and agricultural activity takes place. The annual mean AOD is 0.13 ± 0.05 and 0.15 ± 0.04 at the Haibei and Lhasa sites, respectively; the annual mean α is 0.82 ± 0.51 and -0.15 ± 0.25 , respectively. Both sites have very clean air with low and stable AODs throughout the year, although the windy springtime weather can cause a mild increase in AOD. Frequent cold air surges from Siberia often bring clean air into the region, which wash away particle matter and cause the large day-to-day variations in α . The scatterplots (Figure 4c, first and second plots) and the mean α and AOD (Table 2) with different wind speed show that more large dust aerosol is blown into the atmosphere with increasing wind speed. The southerly wind at Haibei (Table 2) carries a certain amount of aerosol from the upwind agricultural region. From the Himalayas with the highest snow mountain and glacier, the westerly wind with the lowest AOD is cleaner than the other directions at Lhasa (Table 2). There is a much larger range of α over a narrow range of AOD at Haibei (Figure 4c, second plot) than at Lhasa (Figure 4c, first plot), implying the presence of different types of aerosols at the sites. The scatterplot (Figure 4b and Figure 4e, second plot) shows there is an increase in small aerosol particles due to regional biomass burning by the farmer in winter at Haibei, and a faint increase at Lhasa as AOD < 0.1 (Figure 4e, first plot). Nevertheless, the aerosol type is the big dust aerosol at Lhasa in the whole year. Given that Lhasa is located on the Tibetan Plateau with the very sparse population, far away from the influences of urbanization and industrialization, only large continental/dust aerosol particles are present at that site [Yang *et al.*, 1994a; Liu *et al.*, 1997]. The unusually low values of α may be subject to large uncertainties due to the very low AOD values [Jeong *et al.*, 2005].

3.4. Forest Ecosystem

[13] Figure 5 shows results from three sites located in forest ecosystems ranging from northern temperate forests to southern tropical forests. The Beijing Forest site with an elevation of 1130 m is a warm temperate forest ecosystem in the Yanshan Mountain at northern China. The annual mean AOD and α at this site are 0.22 ± 0.09 and 0.82 ± 0.39 , respectively. The seasonal variations of AOD and α are similar to those from the other sites in northern/northeastern China and their magnitudes fall somewhere between those from the northeastern ecosystem sites (Sanjiang, Hailun and Changbai Mt.) and the northern desert sites (Shapotou and Ordos). During autumn and winter, fossil fuel and biomass burning generates smoke and soot aerosols [Cao *et al.*,

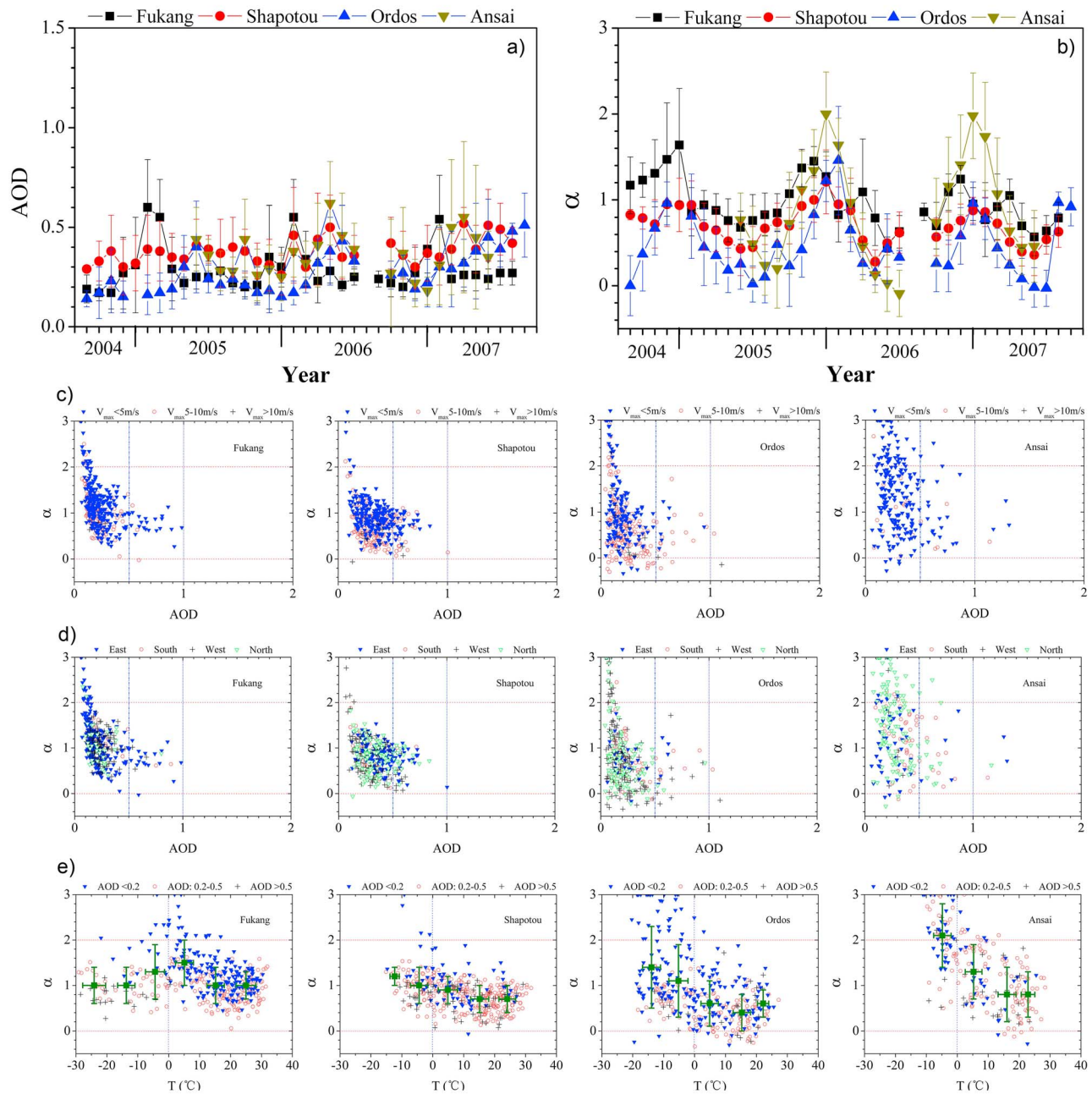


Figure 3. Same as Figure 2 but for the four CERN sites located in an arid region of northern China. The sites are Fukang (oasis), Ordos (sandy grassland), Shapotou (desert), and Ansai (farmland).

2005], which reduces the size of the dominant aerosol particles. During spring and summer, dust storm transportation [Zhou *et al.*, 2004] and local soil dust emission increase both AOD and the size of dominant aerosol particles. The scatterplot (Figure 5c, first plot) shows α as similar functions of AOD when $V_{max} > 5$ m/s and $V_{max} < 5$ m/s. The site has good representative in the region. Figure 5d (first plot) and Table 2 show that the mean AOD is higher under the easterly wind than the other directions. The easterly wind always occurs in summer to carry a certain amount of pollutants from the upwind Beijing urban area. Whereas, the northerly wind from the Yanshan Mountain and the Mongolian Plateau is very clean with the lowest AOD. The

scatterplot of α as a function of T for $AOD < 0.2$ (Figure 5e, first plot) and the time series of mean AOD (Figure 5a) show that the aerosol loading from combustion processes increased during the heating season in northern China. At Beijing Forest, AOD is lowest in winter months (Table 1).

[14] The Dinghu Mountain site with an elevation of 300 m, a subtropical evergreen forest ecosystem, is located along the Pearl River Delta and is about 84 km away from Guangzhou in southeast China. This area has a typical monsoon climate. Annual mean AOD and α are 0.66 ± 0.21 and 1.00 ± 0.41 , respectively. The relatively high aerosol loading is a result of the rapid development of regional industrialization [Wu, 2003; Li *et al.*, 2004; Liu *et al.*,

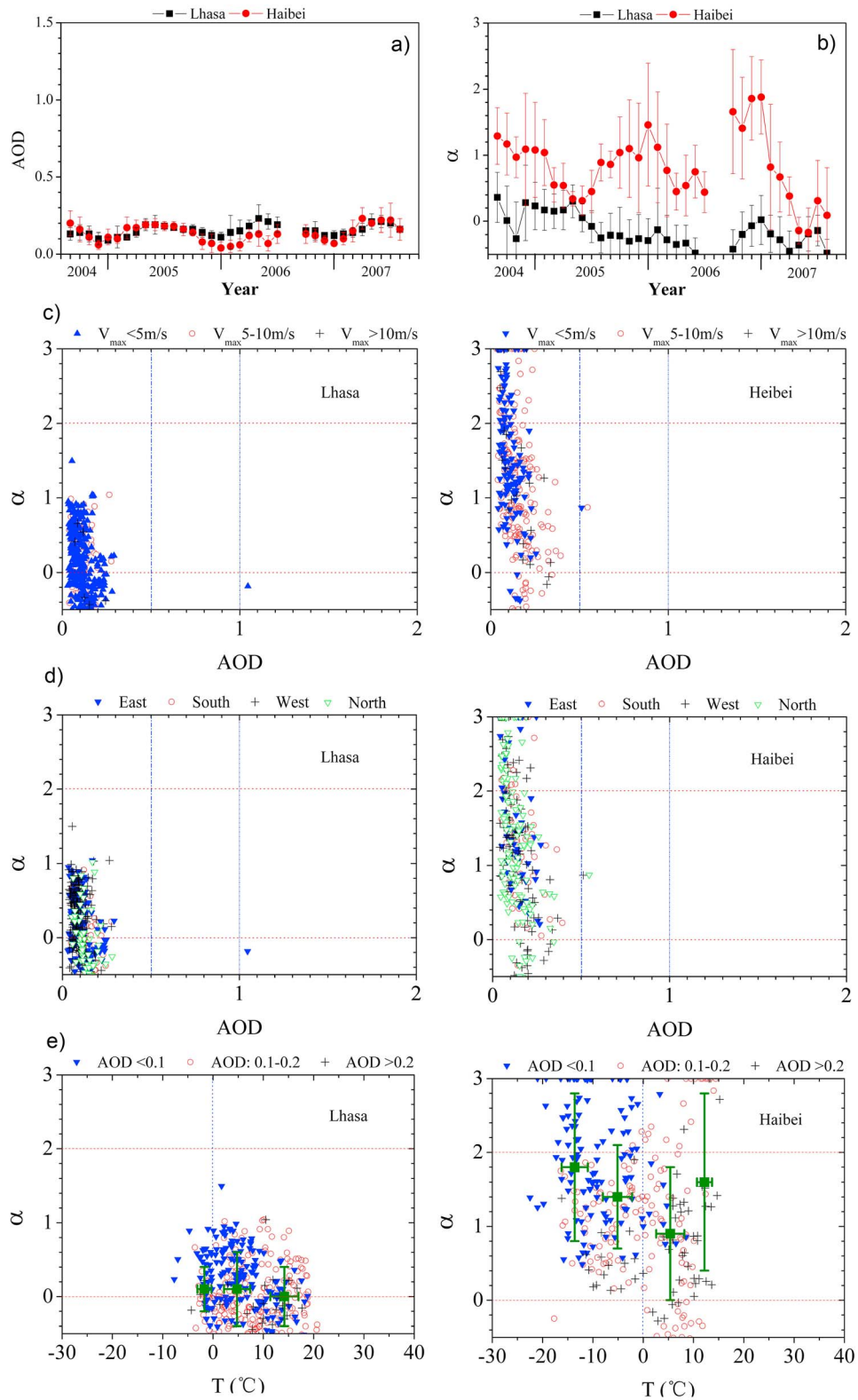


Figure 4. Same as Figure 2 but for the two CERN sites located on the Tibetan Plateau. The sites are Haibei (alpine meadow) and Lhasa (alpine shrub-grassland).

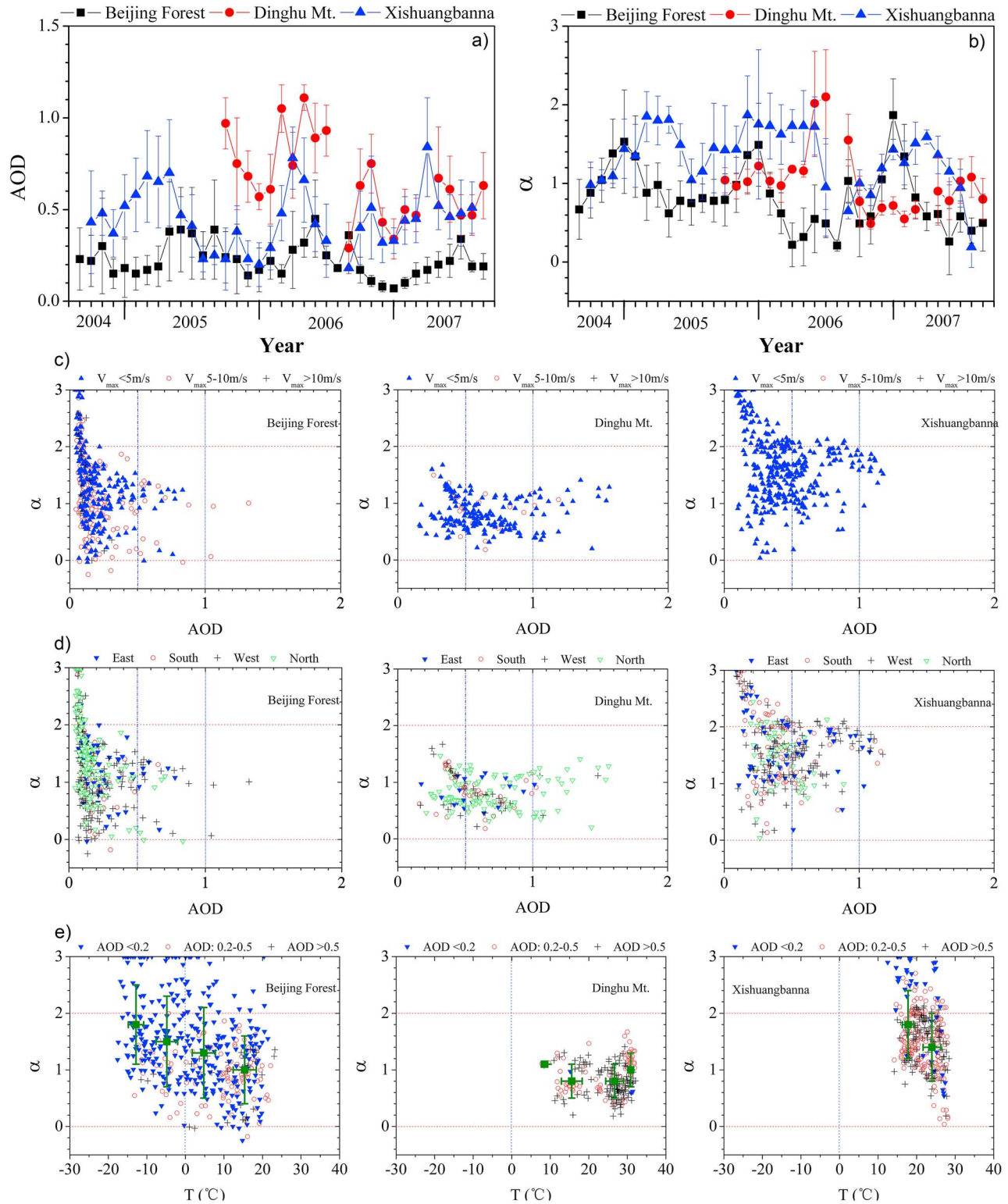


Figure 5. Same as Figure 2 but for the three CERN sites located in a forest ecosystem. The sites are Beijing Forest (a warm temperate forest ecosystem to the west of Beijing City), Dinghu Mountain (a subtropical evergreen forest ecosystem in the Pearl River delta region) and Xishuangbanna (a tropical rain forest ecosystem in Yunnan Province).

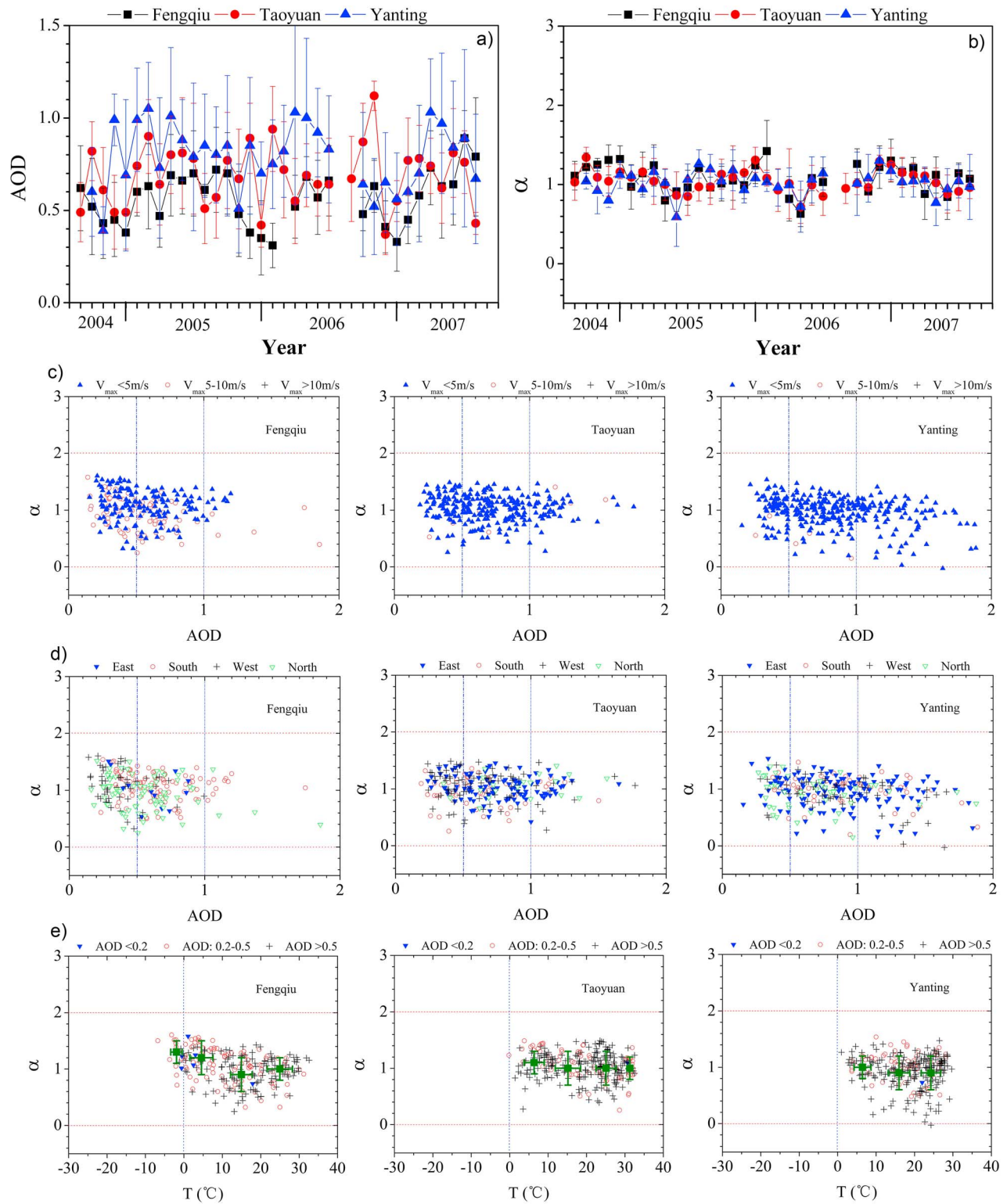


Figure 6. Same as Figure 2 but for the three CERN sites located in a farmland ecosystem. The sites are Fengqiu (on the Huang-huai-hai Plain), Taoyuan (subtropical farmland) and Yanting (in the hilly region of the Sichuan Basin).

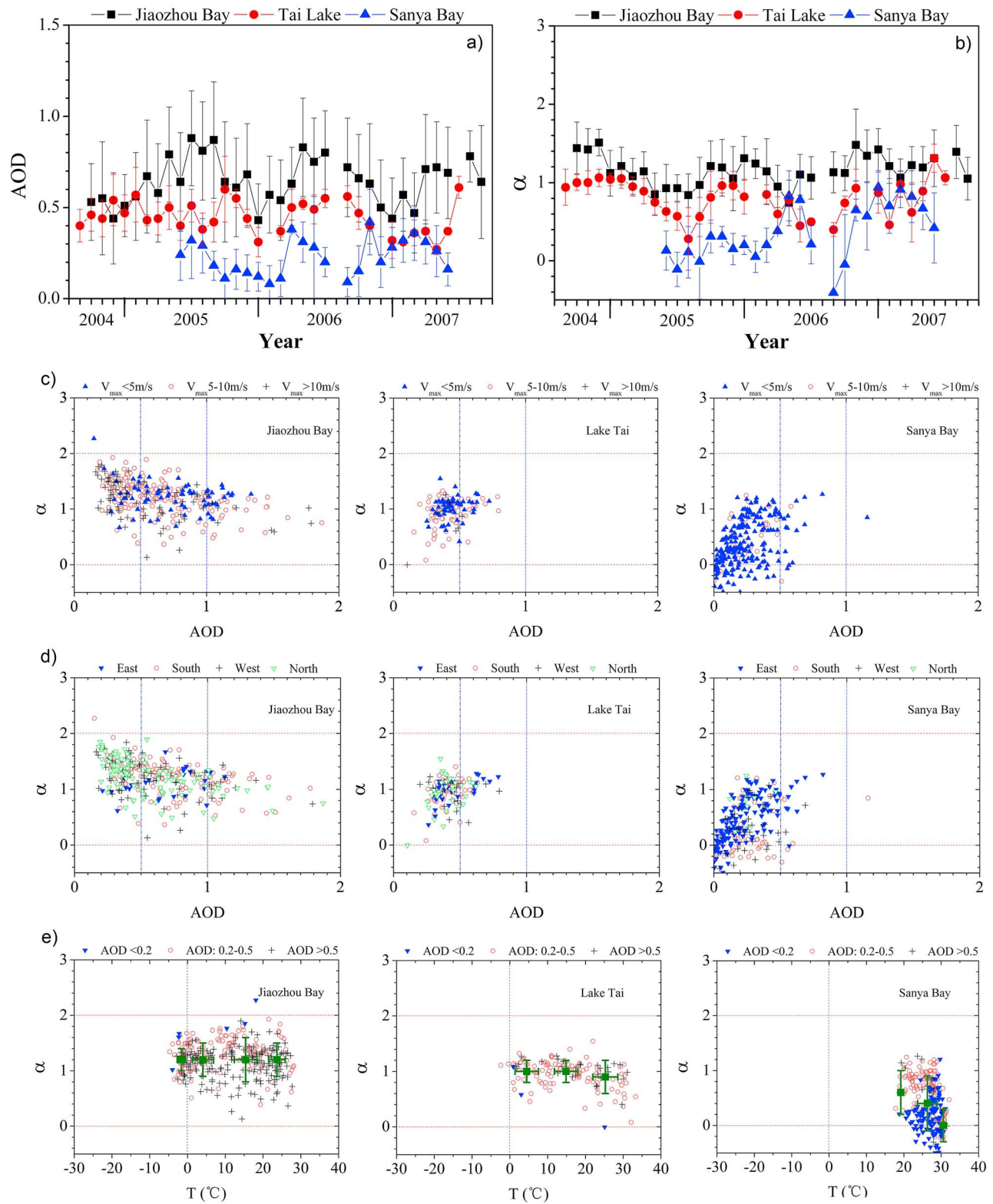


Figure 7. Same as Figure 2 but for the three CERN sites located in a bay or lake ecosystem. The sites are Jiaozhou Bay (on the west coast of the Yellow Sea), Lake Tai (a freshwater lake in the Yangtze River Delta region), and Sanya Bay (a tropical marine bay in the South China Sea).

2003b]. *Ansmann et al.* [2005] observed the aerosol optical properties with Raman lidar and Sun photometer at Xinken (22.6°N, 113.6°E) in the Pearl River Delta, which AOD mean (at 533 nm) was 0.92, and Angstrom exponents mean (for wavelengths 380 to 502 nm) was 0.97 throughout October 2004. The results were close to Dinghu Mountain's. The mean AOD is lower when $V_{\max} > 5$ m/s than $V_{\max} < 5$ m/s (Table 2 and Figure 5c, second plot), which implies the heavy air pollutants are blown away by the relative strong wind. Figure 5c (second plot) and Figure 5d (second plot) show that the wind ($V_{\max} < 5$ m/s) is mainly from the north region with the heavy air pollution and the high AOD [*Liu et al.*, 2003a; *Qi et al.*, 2000].

[15] The Xishuangbanna station is located in the tropical forests of Yunnan Province in southwest China. Annual mean AOD and α are 0.45 ± 0.17 and 1.34 ± 0.39 , respectively. Because there are low wind speed and high temperature in the tropical forest, Figure 5c (third plot) and Figure 5e (third plot) are unavailable. The functions of α and AOD are similar in different wind directions, which implies the observation site has good representative in the region. Figures 5a and 5b show anomalous seasonal variations in AOD and aerosol type. Dense fog frequently occurs in the region, especially during autumn and winter [*Li et al.*, 1992; *Huang et al.*, 2000], resulting in fewer measurements taken at the site. Fog of a certain thickness can remove some amount of large hygroscopic aerosols from the atmosphere, which leads to a decrease in AOD and an increase in α . Suspended fog droplets are generally indistinguishable from haze droplets so the presence of large fog droplets can lead to an increase in AOD and a decrease in α . During the rainy season from May to October, a large amount of aerosol is removed from the atmosphere which reduces AOD. During the dry spring season, AOD and α are at their highest, which implies large emissions of smoke and soot due to biomass burning which is most active in the region and the whole of southeast Asia during this time [*Wu et al.*, 2004; *Tang et al.*, 2003; *Liu et al.*, 1999].

3.5. Farmland Ecosystem

[16] Figure 6 shows the aerosol optical properties at the three sites located in areas dominated by farmland in the eastern/central/southern parts of China. Annual mean AODs at Fengqiu, Taoyuan and Yanting are 0.56 ± 0.14 , 0.69 ± 0.17 and 0.79 ± 0.17 , respectively. AODs at these locations are much higher than in more remote areas because of industrial and agricultural development and human activities in this part of China [*Luo et al.*, 2000]. The annual mean α is approximately equal to 1 with a standard deviation of ~ 0.16 for these stations. α does not obviously increase in the harvest seasons in three main agricultural regions. This may reflect the implementation of a policy by the regional government for the comprehensive utilization of crop stalks, so that smoke aerosol emissions from biomass burning is minimized [*Wu et al.*, 2001; *Guan et al.*, 2005]. More mineral dust aerosols and anthropogenic sulphate aerosols are emitted in eastern China, southern China and the Sichuan Basin [*Tian et al.*, 2005; *Wu et al.*, 2002; *Guan et al.*, 2005], due to intensive farming and industrial activities and the exposure of bare soil. The day-to-day variation of AOD is large, and its seasonal dependence is irregular (Figure 6a). During winter and spring, weather patterns

instigating serious pollution events usually occur in Hunan Province [*Xiong et al.*, 2003; *Zhang et al.*, 2003a] and over the Sichuan Basin [*Liu et al.*, 2003b]. Figure 6d (first, second and third plots) and Table 2 show that the clean westerly wind at Fengqiu, the southerly and westerly winds at Taoyuan, and the northerly wind at Yanting always wash away the air pollutants, that the southerly wind at Fengqiu, the northerly and easterly winds at Taoyuan, and the southerly wind at Yanting carry the heavy air pollutants from the upwind industrial and urban regions. Figure 6e (first plot) shows that there is only a slight increase in α (AOD < 0.5) as T decreased at Fengqiu, which also implies the influence of combustion processes on the aerosol types during the heating season in northern China.

3.6. Bay and Lake Ecosystems

[17] Figure 7 shows the seasonal variations of AOD and α along the east/south coast of China. The annual mean AODs at the Jiaozhou Bay, Tai Lake and Sanya Bay sites are 0.64 ± 0.13 , 0.45 ± 0.09 and 0.23 ± 0.10 , respectively, and the annual mean α were 1.16 ± 0.19 , 0.80 ± 0.24 and 0.39 ± 0.38 , respectively. Of the three sites, AODs are highest at Jiaozhou Bay because of rapid industrial development and an increase in human activities in that area. An increase in aerosol emissions, especially sulphate aerosols along the eastern coastal area and northern China, has been reported [*Luo et al.*, 2000; *Tian et al.*, 2005]. Dust and continental pollution transport from spring to summer contribute to large AODs with substantial standard deviations [*Yang et al.*, 1994b; *Xiao et al.*, 1998; *Sheng et al.*, 2005], while influxes of cold air and clean ocean air alternately wash atmospheric pollution out of the atmosphere and decrease AODs during the winter and fall seasons in the northern region. The westerly and northerly winds are strong but not clean with relative high AOD (Table 2 and Figures 7c (first plot) 7d (first plot)), which indicates the air pollutants from the upwind industrial and agriculture areas replace the local heavy air pollutants. Aerosol pollution is also strong at Tai Lake because the region is dotted with thousands of small privately owned factories emitting huge amounts of pollutants [*Liu et al.*, 2003a; *Zhang et al.*, 2003b]. The small seasonal variations in AOD and α at Tai Lake show that regional aerosol emissions and aerosol components are relatively stable (Table 1). Local sources of emissions include soil, coal combustion, metallurgical and automobile exhaust, and waste incineration [*Xu et al.*, 2002; *Zhou et al.*, 2006]. The easterly wind with high AOD (Table 2) is from the flourishing industrial and urban areas in the Yangtze River Delta region. Large particles, such as soil dust and anthropogenic sulphates, are dominant. Another research group, *Xia et al.* [2007] and *Lee et al.* [2010] also observed the similar seasonal variation and aerosol hygroscopic in the Yangtze Delta region. The daily AOD mean was markedly higher in two papers [*Xia et al.*, 2007; *Lee et al.*, 2010] than the AOD mean around noon in the observation, but we checked the point to point AOD values nearly equal in two experiments. The most southern site, Sanya Bay controlled by the tropical marine monsoon climate, is very clean and large sea salt particles dominate there [*Wu*, 1995; *Wu et al.*, 1996]. During spring, the transition period from the monsoon season, some aerosols originate from Hainan Island so that AOD and α rise (Table 1 and Figures 7a and 7b).

Figures 7c (third plot) and 7d (third plot) show the function of α increasing with AOD is very different from the other continental sites'. The easterly and southerly winds from South China Sea are with relative low AOD (Table 2).

4. Conclusions

[18] In this study, Chinese Sun Hazemeter Network and meteorological data were analyzed in order to examine aerosol optical properties and aerosol types over different ecosystems in China. The annual mean AOD at 500 nm averaged over regions where anthropogenic aerosols are commonly found, e.g., the central/eastern, southern and eastern coastal areas, is 0.60, which is about 3 times more than the regional background mean value over relatively remote dry-clean regions in China (mean AOD~0.23). Similar monthly and seasonal variations of AODs and aerosol types were found from measurements taken over northern and southern China. Main conclusions are as follows:

[19] 1. During spring, dust is the dominant aerosol over northern desert and arid regions. However, dust aerosols transported by dust storms result in an increase in AOD and coarse particle size throughout eastern and southeastern China.

[20] 2. During the humid summer season, hygroscopic sulphate aerosols increase AODs and particle sizes over the central/eastern, southern and eastern coastal areas.

[21] 3. During autumn and winter, relatively thick vegetation and ice-snow coverage limits the emission of soil dust so that AOD decreases in northern China. The majority of observation sites are under the influence of biomass and fossil fuel burning which produce heavy loadings of fine-mode aerosols, smoke and soot.

[22] 4. In the central/eastern, southern and eastern coastal areas, the amount of fine-mode particles remains constant due to environmental regulations and economic measures reducing stalk combustion. Many sites show a mix of sulphate aerosols, mineral aerosols, and smoke aerosols throughout the year.

[23] 5. A small amount of dust and sea salt aerosols are detected over the Tibetan Plateau and at Hainan Island. At the tropical rain forest site, the seasonal and monthly variations of aerosol properties are complicated due to regional dense fog and strong biomass burning in southeast Asia.

[24] **Acknowledgments.** This work was partly supported by the Project of Field Station Network of the Chinese Academy of Sciences, the National Natural Science Foundation of China (40525016; 40675037; 40520120071), and the special project of the Chinese Academy of Sciences (XDA05100100). The authors are grateful to NASA/GSFC and the CERN stations managed by the Chinese Academy of Sciences for their contribution to this research.

References

Alfaro, S. C., et al. (2003), Chemical and optical characterization of aerosols measured in spring 2002 at the ACE-Asia supersite, Zhenbeitai, China, *J. Geophys. Res.*, *108*(D23), 8641, doi:10.1029/2002JD003214.

Ansmann, A., R. Engelmann, D. Althausen, U. Wandinger, M. Hu, and Y. Zhang (2005), High aerosol load over the Pearl River Delta, China, observed with Raman lidar and Sun photometer, *Geophys. Res. Lett.*, *32*, L13815, doi:10.1029/2005GL023094.

Cao, G., X. Zhang, D. Wang, and F. Zheng (2005), Inventory of atmospheric pollutants discharged from biomass burning in China continent (in Chinese), *China Environ. Sci.*, *25*(4), 389–393.

Christopher, L., and TRACE-P Science Team (2003), Preface to the NASA Global Tropospheric Experiment Transport and Chemical Evolution Over the Pacific (TRACE-P): Measurements and analysis, *J. Geophys. Res.*, *108*(D20), 8780, doi:10.1029/2003JD003851.

Dubovik, O., B. N. Holben, T. F. Eck, A. Smirnov, Y. J. Kaufman, M. D. King, D. Tanre, and I. Slutsker (2002), Variability of absorption and optical properties of key aerosol types observed in worldwide locations, *J. Atmos. Sci.*, *59*, 590–608, doi:10.1175/1520-0469(2002)059<0590:VOAAOP>2.0.CO;2.

Eck, T. F., et al. (2005), Columnar aerosol optical properties at AERONET sites in central eastern Asia and aerosol transport to the tropical mid-Pacific, *J. Geophys. Res.*, *110*, D06202, doi:10.1029/2004JD005274.

Forster, P., et al. (2007), Changes in atmospheric constituents and in radiative forcing, in *Climate Change 2007: The Physical Science Basis*, pp. 131–216, Cambridge Univ. Press, New York.

Gai, C., X. Li, and F. Zhao (2006), Mineral aerosol properties observed in the northwest region of China, *Global Planet. Change*, *52*, 173–181, doi:10.1016/j.gloplacha.2005.10.003.

Guan, H., P. Chen, S. Gong, and D. Zhang (2005), Characteristics of air quality and preventing and curing countermeasures of air pollution in cities of Henan Province (in Chinese), *Areal Res. Dev.*, *24*(2), 125–128.

Huang, J., Z. Li, Y. Huang, and Y. Huang (2000), A three-dimensional model study of complex terrain (Xishuangbanna) fog (in Chinese), *Chin. J. Atmos. Sci.*, *24*(6), 821–834.

Huebert, B. J., T. Bates, P. B. Russell, G. Shi, Y. J. Kim, K. Kawamura, G. Carmichael, and T. Nakajima (2003), An overview of ACE-Asia: Strategies for quantifying the relationships between Asian aerosols and their climatic impacts, *J. Geophys. Res.*, *108*(D23), 8633, doi:10.1029/2003JD003550.

Jeong, M. J., Z. Li, D. A. Chu, and S.-T. Tsay (2005), Quality and compatibility analyses of global aerosol products derived from the advanced very high resolution radiometer and Moderate Resolution Imaging Spectroradiometer, *J. Geophys. Res.*, *110*, D10S09, doi:10.1029/2004JD004648.

Kim, D., B. Sohn, T. Nakajima, T. Takamura, B. Choi, and S. Yoon (2004), Aerosol optical properties over East Asia determined from ground-based sky radiation measurements, *J. Geophys. Res.*, *109*, D02209, doi:10.1029/2003JD003387.

Kim, S., S. Yoon, J. Kim, and S. Kim (2007), Seasonal and monthly variations of columnar aerosol optical properties over East Asia determined from multi-year MODIS, LIDAR, and AERONET Sun/sky radiometer measurements, *Atmos. Environ.*, *41*(8), 1634–1651, doi:10.1016/j.atmosenv.2006.10.044.

Lee, K. H., Z. Li, M. S. Wong, J. Xin, Y. Wang, W.-M. Hao, and F. Zhao (2007), Aerosol single scattering albedo estimated across China from a combination of ground and satellite measurements, *J. Geophys. Res.*, *112*, D22S15, doi:10.1029/2007JD009077.

Lee, K. H., Z. Li, M. C. Cribb, J. Liu, L. Wang, Y. Zheng, X. Xia, H. Chen, and B. Li (2010), Aerosol optical depth measurements in eastern China and a new calibration method, *J. Geophys. Res.*, *115*, D00K11, doi:10.1029/2009JD012812.

Lelieveld, J., et al. (2001), The Indian Ocean experiment: Widespread air pollution from south and south-east Asia, *Science*, *291*(5506), 1031–1036, doi:10.1126/science.1057103.

Lewis, E. R., and S. E. Schwartz (2004), *Sea Salt Aerosol Production: Mechanisms, Methods, Measurements and Models—A Critical Review*, *Geophys. Monogr. Ser.*, vol. 152, 413 pp., AGU, Washington, D. C.

Li, C., K. A. Lau, J. Mao, and A. Chen (2004), An aerosol pollution episode in Hong Kong with remote sensing products of MODIS and LIDRA (in Chinese), *J. Appl. Meteorol. Sci.*, *15*(6), 641–650.

Li, Z. (2004), Aerosol and climate: A perspective from East Asia, in *Observation, Theory, and Modeling of the Atmospheric Variability*, edited by D. Zhu, pp. 501–525, World Sci., Hackensack, N. J., doi:10.1142/9789812791139_0025.

Li, Z., L. Zhong, and X. Yu (1992), The temporal-spatial distribution and physical structure of land fog in southwest China and the Changjiang River basin (in Chinese), *Acta Geogr. Sin.*, *47*(3), 242–251.

Li, Z., F. Niu, K.-H. Lee, J. Xin, W.-M. Hao, B. Nordgren, Y. Wang, and P. Wang (2007a), Validation and understanding of Moderate Resolution Imaging Spectroradiometer aerosol products (C5) using ground-based measurements from the handheld Sun photometer network in China, *J. Geophys. Res.*, *112*, D22S07, doi:10.1029/2007JD008479.

Li, Z., et al. (2007b), Preface to special section on East Asian Studies of Tropospheric Aerosols: An International Regional Experiment (EAST-AIRE), *J. Geophys. Res.*, *112*, D22S00, doi:10.1029/2007JD008853.

Li, Z., K.-H. Lee, Y. Wang, J. Xin, and W.-M. Hao (2010), First observation-based estimates of cloud-free aerosol radiative forcing across China, *J. Geophys. Res.*, *115*, D00K18, doi:10.1029/2009JD013306.

- Li, Z., et al. (2011), East Asian Studies of Tropospheric Aerosols and Impact on Regional Climate (EAST-AIRC): An overview, *J. Geophys. Res.*, 116, D00K34, doi:10.1029/2010JD015257.
- Liang, S., B. Zhong, and H. Fang (2006), Improved estimation of aerosol optical depth from MODIS imagery over land surfaces, *Remote Sens. Environ.*, 104, 416–425, doi:10.1016/j.rse.2006.05.016.
- Liu, G., J. Mao, and C. Li (2003a), Optical depth study on atmospheric aerosol in Yangtze River delta region (in Chinese), *Shanghai Environ. Sci.*, 22, Suppl., 58–63.
- Liu, G., A. Zhu, X. Liu, Z. Yuan, J. Chen, K. A. Lau, J. Mao, and C. Li (2003b), Characteristics of distribution and seasonal variation of aerosol optical depth in eastern China with MODIS products, *Chin. Sci. Bull.*, 48(22), 2488–2495.
- Liu, H., X. Zhang, and Z. Shen (1997), The chemical composition and concentration of atmospheric aerosol at Wudaoliang and its seasonal variation (in Chinese), *Plateau Meteorol.*, 16(2), 122–129.
- Liu, H. Y., W. L. Chang, J. O. Samuel, L. Y. Chan, and M. H. Joyce (1999), On springtime high ozone events in the lower troposphere from southeast Asian biomass burning, *Atmos. Environ.*, 33(15), 2403–2410, doi:10.1016/S1352-2310(98)00357-4.
- Liu, J., et al. (2010), Validation of multi-angle imaging spectroradiometer aerosol products in China, *Tellus, Ser. B*, 62, 117–124, doi:10.1111/j.1600-0889.2009.00450.x.
- Luo, Y., D. Lü, and W. Li (2000), The characteristics of atmospheric aerosol optical depth variation over China in recent 30 years (in Chinese), *Chin. Sci. Bull.*, 45, 1328–1334, doi:10.1007/BF03182914.
- Mao, J., J. Zhang, and M. Wang (2002), Summary comment on research of atmospheric aerosol in China (in Chinese), *Acta Meteorol. Sin.*, 60(5), 625–634.
- Nakajima, T., et al. (2003), Significance of direct and indirect radiative forcings of aerosols in the East China Sea region, *J. Geophys. Res.*, 108(D23), 8658, doi:10.1029/2002JD003261.
- Nakajima, T., et al. (2007), Overview of the Atmospheric Brown Cloud East Asian Regional Experiment 2005 and a study of the aerosol direct radiative forcing in East Asia, *J. Geophys. Res.*, 112, D24S91, doi:10.1029/2007JD009009.
- Penner, J. E., et al. (2001), *Aerosols, their direct and indirect effects, in Climate Change 2001: The Scientific Basis*, pp. 291–335, Cambridge Univ. Press, New York.
- Qi, S., G. Sheng, and Z. Ye (2000), Study on organic pollutant background in aerosols in Pearl River delta area (in Chinese), *China Environ. Sci.*, 20(3), 225–228.
- Qiu, J., D. Lu, H. Chen, G. Wang, and G. Shi (2003), Modern research progresses in atmospheric physics (in Chinese), *Chin. J. Atmos. Sci.*, 27(4), 628–652.
- Seinfeld, J. H., and S. N. Pandis (1998), *Atmospheric Chemistry and Physics: From Air Pollution to Climate Change*, 1326 pp., John Wiley, Hoboken, N. J.
- Seinfeld, J. H., et al. (2004), ACE-ASIA: Regional climatic and atmospheric chemical effects of Asian dust and pollution, *Bull. Am. Meteorol. Soc.*, 85(3), 367–380, doi:10.1175/BAMS-85-3-367.
- Sheng, L., Z. Guo, and H. Gao (2005), Preliminary study on element composition and source apportionment of atmospheric aerosol over Bohai Sea (in Chinese), *Environ. Monit. China*, 21(1), 16–20.
- Streets, D. G., and K. Aunan (2005), The importance of China's household sector for black carbon emissions, *Geophys. Res. Lett.*, 32, L12708, doi:10.1029/2005GL022960.
- Streets, D. G., S. Gupta, S. T. Waldhoff, M. Q. Wang, T. C. Bond, and Y. Bo (2001), Black carbon emissions in China, *Atmos. Environ.*, 35, 4281–4296, doi:10.1016/S1352-2310(01)00179-0.
- Streets, D. G., et al. (2003), An inventory of gaseous and primary aerosol emissions in Asia in the year 2000, *J. Geophys. Res.*, 108(D21), 8809, doi:10.1029/2002JD003093.
- Streets, D. G., T. C. Bond, T. Lee, and C. Jang (2004), On the future of carbonaceous aerosol emissions, *J. Geophys. Res.*, 109, D24212, doi:10.1029/2004JD004902.
- Tang, Y., et al. (2003), The influences of biomass burning during TRACE-P experiment identified by the regional chemical transport model, *J. Geophys. Res.*, 108(D21), 8824, doi:10.1029/2002JD003110.
- Tian, H., J. Ma, W. Li, and H. Liu (2005), Simulation of forcing of sulfate aerosol on direct radiation and its climate effect over middle and eastern China (in Chinese), *J. Appl. Meteorol. Sci.*, 16(3), 322–333.
- Wang, L., J. Xin, Y. Wang, Z. Li, P. Wang, G. Liu, and T. Wen (2007), Validation of MODIS aerosol products by CSHNET over China, *Chin. Sci. Bull.*, 52(12), 1708–1718, doi:10.1007/s11434-007-0222-0.
- Wu, D. (1995), The distribution characteristics of water-soluble composition of atmospheric aerosol over north of the South China Sea (in Chinese), *Sci. Atmos. Sin.*, 19(5), 615–622.
- Wu, D. (2003), A review and outlook on the aerosol study over south China (in Chinese), *J. Trop. Meteorol.*, 19, Suppl., 145–151.
- Wu, D., J. You, and Y. Guan (1996), The distribution feature of giant sea-salt nucleus in atmosphere over Yongxing (Xisha Islands) during the northeast winter monsoon, *J. Trop. Meteorol.*, 12(2), 122–129.
- Wu, J., W. Jiang, H. Liu, and J. Tang (2002), Simulation of the direct and indirect radiative effects of sulfate aerosol (in Chinese), *Acta Sci. Circumstantiae*, 22(2), 129–134.
- Wu, J., W. Jiang, and X. Chen (2004), Simulation of effects to tropospheric ozone over south east Asia and south China from biomass burning (in Chinese), *Environ. Sci.*, 25(2), 1–6.
- Wu, L., J. Chen, and X. Zhu (2001), Straw-burning in rural areas of China: Causes and controlling strategy (in Chinese), *China Popul. Resour. Environ.*, 11(51), 110–112.
- Xia, X., H. Chen, and P. Wang (2004), Aerosol properties in a Chinese semi-arid region, *Atmos. Environ.*, 38, 4571–4581, doi:10.1016/j.atmosenv.2004.04.015.
- Xia, X., Z. Li, B. Holben, P. Wang, T. Eck, H. Chen, M. Cribb, and Y. Zhao (2007), Aerosol optical properties and radiative effects in the Yangtze Delta region of China, *J. Geophys. Res.*, 112, D22S12, doi:10.1029/2007JD008859.
- Xiao, H., R. C. Gregory, and Z. Yang (1998), A modelling evaluation of the impact of mineral aerosols on the particulate sulfate formation in east Asia (in Chinese), *Sci. Atmos. Sin.*, 22(3), 343–353.
- Xin, J., S. Wang, Y. Wang, J. Yuan, W. Zhang, and C. Liu (2005), Optical properties and size distribution of dust aerosols over the Tengger Desert in northern China, *Atmos. Environ.*, 39, 5971–5978, doi:10.1016/j.atmosenv.2005.06.027.
- Xin, J., Y. Wang, Z. Li, P. Wang, S. Wang, T. Wen, and Y. Sun (2006), Introduction and calibration of the Chinese Sun Hazemeter Network (in Chinese), *Environ. Sci.*, 27(9), 1697–1702.
- Xin, J., et al. (2007), AOD and Angstrom exponent of aerosols observed by the Chinese Sun Hazemeter Network from August 2004 to September 2005, *J. Geophys. Res.*, 112, D05203, doi:10.1029/2006JD007075.
- Xiong, M., H. Lu, and F. Wu (2003), Analysis on air quality in major cities of Hunan Province (in Chinese), *J. Nat. Sci. Human Norm. Univ.*, 26(1), 89–92.
- Xiu, X., X. Zhou, Y. Weng, G. Tian, Y. Liu, P. Yan, G. Ding, Y. Zhang, J. Mao, and H. Qiu (2003), Explore aerosol variational field by using MODIS data and ground-based photometer observation (in Chinese), *Chin. Sci. Bull.*, 48(15), 1680–1685.
- Xu, J., M. H. Bergin, X. Yu, G. Liu, J. Zhao, C. M. Carrico, and K. Baumann (2002), Measurement of aerosol chemical, physical and radiative properties in the Yangtze delta region of China, *Atmos. Environ.*, 36, 161–173, doi:10.1016/S1352-2310(01)00455-1.
- Yang, L., M. Wang, G. Lu, and Y. Gong (1994a), The observation and research for the continental aerosol background characteristics in the northern part of the Qinghai-Xizang Plateau (in Chinese), *Plateau Meteorol.*, 13(2), 135–143.
- Yang, S., Y. Yang, and B. Chen (1994b), Input of atmospheric trace elements to the near-China ocean (in Chinese), *Environ. Chem.*, 13(5), 382–388.
- Yu, J., J. Liu, J. Wang, and Y. Zheng (1999), The impact of ecological environment and strategy of sustainable development from ginseng industrial development in the Changbai Mountain region (in Chinese), *Agroenviron. Dev.*, 16(4), 28–30.
- Zhang, G., G. Zeng, Y. Jiang, and H. Liu (2003a), Analysis on the variant characteristics, present situation and origin of acid rain in Hunan Province (in Chinese), *Res. Environ. Sci.*, 16(5), 14–17.
- Zhang, J., Z. Si, J. Mao, and M. Wang (2003b), Remote sensing aerosol optical depth over China with GMS-5 satellite (in Chinese), *Chin. J. Atmos. Sci.*, 27(1), 23–35.
- Zhou, R., H. Liu, and W. Jiang (2004), The study on the transport of dust aerosol in China (in Chinese), *Sci. Meteorol. Sin.*, 24(1), 16–25.
- Zhou, Z., K. Liu, and Y. Sun (2006), Characteristics of elements in PM_{2.5} and sources analysis of PM_{2.5} in rural areas of southern Jiangsu Province (in Chinese), *Res. Environ. Sci.*, 19(3), 24–28.

H. Chen, Y. Sun, L. Wang, P. Wang, Y. Wang, and J. Xin, LAPC, Institute of Atmospheric Physics, Chinese Academy of Sciences, Beijing 100029, China. (xjy@mail.iap.ac.cn)

W. M. Hao and B. L. Nordgren, Fire Sciences Laboratory, USDA Forest Service, Missoula, MT 59808, USA.

Z. Li, Department of Atmospheric and Oceanic Sciences, University of Maryland, College Park, MD 20782, USA.

S. Wang, College of Atmospheric Science, Lanzhou University, Lanzhou 730000, China.